Hepatectomy alters adjuvant anti–PD-1 action in a mouse model of HCC but does not compromise neoadjuvant efficacy

VISUAL ABSTRACT

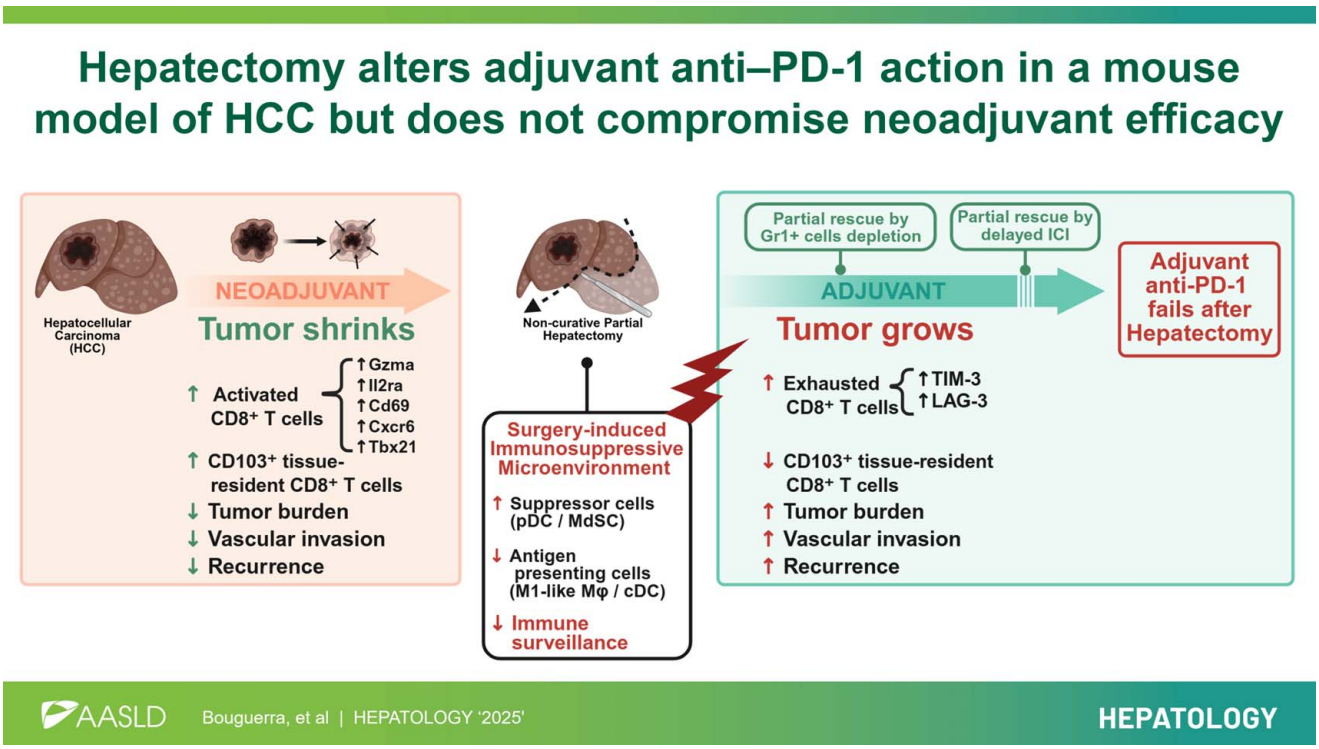

Received: 8 September 2025 | Accepted: 1 October 2025

DOI: 10.1097/HEP.0000000000001575

ORIGINAL ARTICLE

Hepatectomy alters adjuvant anti–PD-1 action in a mouse model of HCC but does not compromise neoadjuvant efficacy

Roqiya Bouguerra[1] | **Sofia El Hajji**[1,2] | **Charles-Henri Wassmer**[1,2] | **Arnaud Bakaric**[3] | **Florence Slits**[1] | **Beat Moeckli**[1,2] | **Laura Rubbia-Brandt**[3] | **Stéphanie Lacotte**[1] | **Christian Toso**[1,2]

[1]Transplantation and Hepatology Laboratory, Department of Surgery, University of Geneva, Geneva, Switzerland

[2]Department of Surgery, Geneva University Hospitals and Faculty of Medicine, Geneva, Switzerland

[3]Clinical Pathology Service, Department of Diagnostics, Geneva University Hospitals, Geneva, Switzerland

Correspondence
Christian Toso, Department of Surgery, Division of Digestive Surgery, University Hospitals of Geneva, Rue Gabrielle-Perret-Gentil 4, Geneva 1205, Switzerland.
Email: christian.toso@hug.ch

Stéphanie Lacotte, Department of Surgery, Transplantation & Hepatology Lab, University of Geneva, Rue Michel-Servet 1, Geneva 1206, Switzerland.
Email: stephanie.lacotte@unige.ch

Abstract

Background and Aims: Immune checkpoint inhibitors have transformed the management of advanced HCC, yet their integration in the perioperative setting remains insufficiently explored. This study aims to investigate the effect of hepatectomy on the tumor microenvironment and assess whether neoadjuvant or adjuvant anti–PD-1 (programmed cell death protein 1) therapy offers improved therapeutic outcomes.

Approach and Results: Using a murine orthotopic HCC model, a non-curative partial hepatectomy was performed, removing a non–tumor-bearing lobe with anti–PD-1 administered as neoadjuvant or adjuvant therapy. In a separate experiment, curative hepatectomy (resection of the tumor-bearing lobe) was performed to evaluate recurrence and survival.

Anti–PD-1 therapy significantly reduced tumor growth in nonsurgical settings ($p = 0.0094$), but its efficacy was lost in the adjuvant setting. This loss correlates with reduced infiltration of effector memory $CD103^+CD8^+$ T cells, increased expression of exhaustion markers (TIM-3 and LAG-3), and accumulation of myeloid-derived suppressor cells. Myeloid-derived suppressor cell depletion at the time of surgery improved adjuvant efficacy ($p = 0.0084$), and delaying adjuvant immune checkpoint inhibitor partially rescued responses, indicating a temporary postoperative immunosuppressive window. By contrast, neoadjuvant anti–PD-1 therapy significantly reduced tumor burden ($p = 0.0005$), enhanced immune cell infiltration, and increased the expression of key activation markers on $CD8^+$ cells (Tbx21, Gzma, Cxcr6, and Cd69). Moreover, neoadjuvant treatment significantly reduced recurrence rates compared with sham treatment (35% vs.

Abbreviations: cDC, conventional dendritic cell; ICI, Immune checkpoint inhibitor; IVIS, in vivo imaging system; MDSC, myeloid-derived suppressor cell; MFI, mean fluorescence intensity; PD-1, programmed cell death protein 1; TIL, tumor-infiltrating lymphocyte; TME, tumor microenvironment.

Roqiya Bouguerra and Sofia El Hajji contributed equally to this work.

Supplemental Digital Content is available for this article. Direct URL citations are provided in the HTML and PDF versions of this article on the journal's website, www.hepjournal.com.

68%, $p = 0.0405$) and improved survival ($p = 0.0373$), which was not achieved with adjuvant therapy.

Conclusions: Partial hepatectomy disrupts antitumor immunity and limits adjuvant immune checkpoint inhibitor efficacy. Neoadjuvant anti–PD-1 immunotherapy offers a superior strategy compared with adjuvant immunotherapy in enhancing immune responses and reducing HCC recurrence.

Keywords: adjuvant, HCC, hepatectomy, immune checkpoint inhibitor, myeloid-derived suppressor cells, neoadjuvant, tumor burden

INTRODUCTION

Immune checkpoint inhibitors (ICIs) have revolutionized the therapeutic landscape of HCC. Given the immunologic complexity of its tumor microenvironment (TME),[1] ICI restores T-cell–mediated antitumor activity through the blockade of inhibitory pathways such as programmed cell death protein 1 (PD-1), programmed cell death protein ligand 1, and cytotoxic T-lymphocyte-associated protein 4.[2] While early systemic therapy, dominated by sorafenib, yielded limited benefit in advanced HCC,[2,3] combination ICI regimens have since achieved superior outcomes in clinical studies, as in IMbrave150 (atezolizumab + bevacizumab),[4] HIMALAYA (durvalumab + tremelimumab),[5] and CARES-310 (camrelizumab + revoceranib)[6] and further confirmed the efficacy of novel ICI combinations.[7] These advances have encouraged the evaluation of ICI at earlier disease stages alongside curative interventions for different solid tumors.[8]

In HCC specifically, recurrence remains a major challenge, affecting over 40% of patients with early-stage HCC within 3 years after resection.[9] Extending ICI with curative treatments may reduce early relapse and enhance immune surveillance to prevent the emergence of new lesions.[10]

Recent clinical trials have evaluated ICI in the adjuvant setting with promising but inconsistent results. IMbrave050 trial showed no difference in recurrence-free survival in patients treated with adjuvant atezolizumab plus bevacizumab after resection compared with active surveillance,[11] whereas Wang et al[10] reported improved outcomes using sintilimab monotherapy (anti–PD-1). Some factors can explain the limited effectiveness of ICI used as an adjuvant therapy. Surgical removal of bulk tumors eliminates the antigenic stimulus needed to prime effective T-cell responses[12] and may also deplete a rich source of tumor-specific infiltrating lymphocyte populations within the TME, thereby limiting the pool of cells necessary for effective ICI.[13] In addition, the impact of adjuvant ICI may be compromised by the surgery-induced immunosuppression.[14]

By contrast, neoadjuvant ICI, administered before surgery while the tumor and its immunogenic milieu are still intact, may offer superior immunologic priming and long-term control. Preclinical models reinforce this concept. In murine breast cancer models, neoadjuvant ICI resulted in greater tumor control and a more robust and durable immune response compared with adjuvant administration.[2] Trials in other cancer types, such as CheckMate 816 in non–small cell lung cancer, support this approach by demonstrating improved pathologic responses and survival.[15] Moreover, evidence from early-phase clinical trials and translational studies has demonstrated that neoadjuvant ICI can induce pathologic responses,[16] remodel the TME, and activate a robust, lasting immune response against HCC.[17]

While both strategies aim to reduce recurrence and improve survival, fundamental questions remain; the optimal timing, therapy combination, and mechanisms of action for perioperative ICI have yet to be defined. Furthermore, it is unclear how factors such as the baseline tumor immune microenvironment, the stress responses to surgery, and the patient's metabolic and health conditions influence the therapeutic outcome.

Considering the promising role of ICI therapy when combined with curative treatments at an early to intermediate stage of HCC, in this study, we hypothesize that neoadjuvant ICI is superior to adjuvant ICI on survival, recurrence, and tumor-immune microenvironment remodeling in HCC in a mouse preclinical HCC model. This work aims to contribute to a better understanding of perioperative immunotherapy strategies and to provide guidance for their clinical application in HCC.

METHODS

Ethics statement and mouse models

All animal experiments were conducted in accordance with Swiss institutional guidelines following the principles

of the ARRIVE (Animals in Research: Reporting In Vivo Experiments) guidelines. The study protocol was reviewed and approved by the ethical committee of the University of Geneva and the Geneva cantonal veterinary authorities (ethical approval reference number: GE321). C57BL/6 mice were kept in the institution's specific pathogen-free animal facility. Humane endpoints were predefined based on body condition, pain level, tumor size, or signs of morbidity. Mice displaying signs of distress or excessive tumor burden were humanely euthanized in accordance with Swiss ethical guidelines. To avoid any influence of sex, only male mice were used in the study. Exact sample sizes (n per group for each figure and panel) are provided in Supplemental Table S2, http://links.lww.com/HEP/K302.

For the induction of HCC, animals were orthotopically injected with 1×10^5 RIL-175 HCC cells suspended in 10 µL of Cultrex Basement Membrane Extract Type 3 (R&D Systems) using a 29G needle under the liver capsule of the right median lobe through a small midline laparotomy. The RIL-175 Luciferase-tagged cell line (RRID:CVCL_B7TK) was kindly gifted by Dr Tim F. Greten [National Cancer Institute, National Institutes of Health, Bethesda, MD] [18,19]. Stable luciferase expression was established by retroviral transduction using a pBABE-luc-puro vector, as previously described [20]. In the extrahepatic model, tumors were established subcutaneously in the dorsal part. Tumor establishment and size were monitored using in vivo bioluminescent imaging with an in vivo imaging system (IVIS, Revvity). Mice were injected intraperitoneally with D-luciferin (300 µg/mouse; MCE) and imaged 5 minutes after injection. Two images were acquired per session with a 3-minute interval between acquisitions. Imaging was performed using an auto exposure time, medium binning, F/Stop 1.2, and a 13×13 cm field of view (FOV C). Quantification was conducted using Living Image 4.8.2 software. Regions of interest were manually drawn over the liver area using a fixed circular template for consistency, and total flux (photons/s) was quantified for each animal and normalized across experiments. The background signal was subtracted using a standardized region of interest placed outside the animal body.

Seven days after the injection, mice with an established HCC tumor were randomized into groups according to bioluminescent imaging values. Partial noncurative left lateral lobe hepatectomy (~35%) was performed, leaving the tumor-bearing lobe in place. Anti–PD-1 antibody (clone RMP1-14, AssayGenie) or its control isotype rat IgG2a (clone 1-1, AssayGenie) was administered intraperitoneally at 200 µg per mouse either 2 and 4 days before surgery (neoadjuvant) or 2 and 4 days after surgery (adjuvant).

In the Gr1$^+$-cells-depleted model, mice received 3 i.p. injections of 200 µg anti-Gr1 antibody (clone RB6-8C5) 2 days before and 1 and 2 days after hepatectomy.

In the recurrence model, curative hepatectomy was performed by the removal of the liver lobe with the tumor mass. Mice were monitored over time and sacrificed on day 70 after HCC cell injection.

Tumor dissociation and sample preparation

Liver tumors were harvested and mechanically minced with sterile razor blades in 2.5 mL of digestion medium per mouse: IMDM supplemented with collagenase IV (LS004188, Worthington, 1.5 mg/mL), hyaluronidase (H3506, Sigma, 1 mg/mL), and DNase I (10104159001, Sigma, 150 µg/mL). Samples were processed on a GentleMACS Dissociator (Miltenyi Biotec) using the following programs: pre-digestion for 40 seconds, 40 minutes incubation at 37 °C, followed by an additional digestion for 40 seconds, then for 1 minute. Digests were diluted with 4 mL of DMEM, filtered through 70 µm strainers, and washed. 1×10^6 viable cells per sample were used for downstream experiments.

Flow cytometry

Cells were incubated with LIVE/DEAD Fixable Near-IR Dead Cell Stain (Invitrogen). After washing, surface staining was performed using antibodies targeting lymphoid or myeloid markers (antibody panel and fluorophore details are available in the Supplemental Table S1, http://links.lww.com/HEP/K302). Cells were fixed in FluoroFix (BioLegend), washed, and permeabilized using Perm/Wash buffer (BD Biosciences). Intracellular staining was carried out in Perm/Wash buffer, followed by washing and final resuspension in 300 µL of PBS.

Acquisition was performed using a Cytek Aurora or Beckman Coulter CytoFLEX flow cytometer. Data were analyzed using SpectroFlo v3.0 and FlowJo v10.9 software. Gating strategies were standardized across samples (Supplemental Figures S1 and S2, http://links.lww.com/HEP/K302). Debris and doublets were excluded, and live single CD45$^+$ immune cells were gated for further analysis. Results are presented either as the percentage of cells within a defined population or as mean fluorescence intensity (MFI), as appropriate.

Histology and immunohistochemistry

Liver and tumor samples were collected, fixed in 4% neutral buffered formalin, dehydrated and embedded in paraffin. Sections of 5 µm thickness were cut, mounted on glass slides, deparaffinized, and stained with hematoxylin & eosin for histopathological evaluation.

For immunohistochemistry, antigen retrieval was performed using antigen unmasking solution (0.01 M citrate buffer pH = 6, 0.5% Tween) using a pressure cooker for 10 minutes at high pressure (80 kPa). Slides were incubated in hydrogen peroxide (3%) and blocked with 0.5% bovine serum albumin in TBS, Tween 0.1%. Samples were then incubated overnight at 4 °C with the appropriate primary antibody (anti-CD45 antibody (clone D3F8Q, Cell Signaling), anti-CD34 (EP373Y, Abcam), anti-Lyv-1 (AF2125, R&D Systems), and anti-CD8 (D4W2Z, Cell Signaling)). All slides were incubated with the appropriate HRP SignalStain Boost IHC Detection Reagent (Cell Signaling). Signal detection was performed using DAB chromogen substrate (ThermoFisher). Images were acquired using the Zeiss Axioscan-Z1 Microscope slide scanner (ZEN 2 Blue Edition v1.0 software), and quantification was performed using QuPath v0.5.1. An expert pathologist blindly assessed slides. CD8+ T cells were counted manually within the hotspot, defined as the area of highest density, using 1 high-power field at ×20 magnification. Lymphovascular invasion was assessed on whole-slide examination of hematoxylin & eosin–stained sections. In cases where the evaluation on hematoxylin & eosin was equivocal, immunohistochemistry with CD34 and Lyve-1 was performed to confirm vascular or lymphatic invasion.

RNA sequencing and quantitative PCR

$CD8^+$ T cells were isolated from tumor-infiltrating lymphocytes (TILs) using a magnetic bead cell enrichment kit ($CD8a^+$ T Cell Isolation Kit, Miltenyi Biotec). Total RNA was extracted using the ReliaPrepTM RNA Miniprep system kit (Promega).

RNA sequencing was performed at the iGE3 Genomics Platform of the University of Geneva. The library was prepared using the TruSeqHT stranded mRNA ligation protocol, and sequencing was performed on an Illumina NovaSeq 6000. The differential expression analysis was performed with the R/Bioconductor-DESEq. 2 v.1.46.0 package.

cDNA was synthesized by extending a mix of random primers with the High-Capacity cDNA Reverse Transcription Kit in the presence of RNAase Inhibitor (Applied Biosystems). The relative quantity of each transcript (2-ΔΔCt method) was normalized to the expression of EEF1, HPRT, and GAPDH.

Statistical analysis

All statistical analyses were performed using GraphPad Prism v10.2.0 software. Data are presented as median with IQR. Comparisons between 2 groups were made using an unpaired 2-tailed Student *t* test or Mann-Whitney *U* test as appropriate. For comparisons between more than 2 groups, a 1-way ANOVA or a Kruskal-Wallis test was used as appropriate. *p* values < 0.05 were considered statistically significant.

RESULTS

Surgical resection impacts the efficacy of adjuvant anti–PD-1 immunotherapy in an HCC murine model

To assess the impact of partial liver resection on ICI efficacy, we established orthotopic tumors in C57BL/6 mice by intrahepatic injection of luciferase-expressing RIL-175 cells. Mice were then randomized into 4 experimental groups to receive either no treatment, 2 anti–PD-1 ICI injections, partial hepatectomy alone, or followed by 2 anti–PD-1 ICI injections (Figure 1A).

Anti–PD-1 alone significantly reduced tumor burden compared with untreated control ($p = 0.0094$; Figures 1B–D), confirming the efficacy of the treatment on HCC tumors. However, when combined with surgical resection, ICI failed to control tumor growth, suggesting that surgery impairs treatment efficacy. Liver-tumor mass-to-body weight ratios were also significantly improved in mice receiving the ICI treatment with no resection ($p = 0.0262$; Figure 1E), but not in those treated in the adjuvant setting, supporting the loss of treatment efficacy after surgery.

Flow cytometry data of TILs revealed a significant increase in $CD103^+CD8^+$ T cells in the nonsurgical ICI-treated group compared with both the nonsurgical isotype-treated group and adjuvant-treated group ($p = 0.020$ and $p = 0.010$, respectively; Figure 1F). CD103 is known to be expressed on tissue-resident memory T cells, contributing to antitumor immunity and associated with improved prognosis in cancer.[21] The expression of the exhaustion marker LAG-3 was also significantly decreased in the nonsurgical treated group ($p = 0.0426$; Figure 1G), while TIM-3 levels were also lower, though the difference did not reach statistical significance ($p = 0.1419$; Figure 1H), suggesting a more functional cytotoxic T-cell phenotype. No differences in either exhaustion markers were observed between the surgical groups with or without anti–PD-1, indicating that surgery affects the key players of ICI-mediated immunity.

Anti–PD-1 immunotherapy delivery is not altered by surgery

Anti–PD-1 MFI of $CD8^+$ TILs was lower in ICI-treated compared with the isotype control mice (Figure 2A). Although the anti–PD-1 clone used for flow cytometry

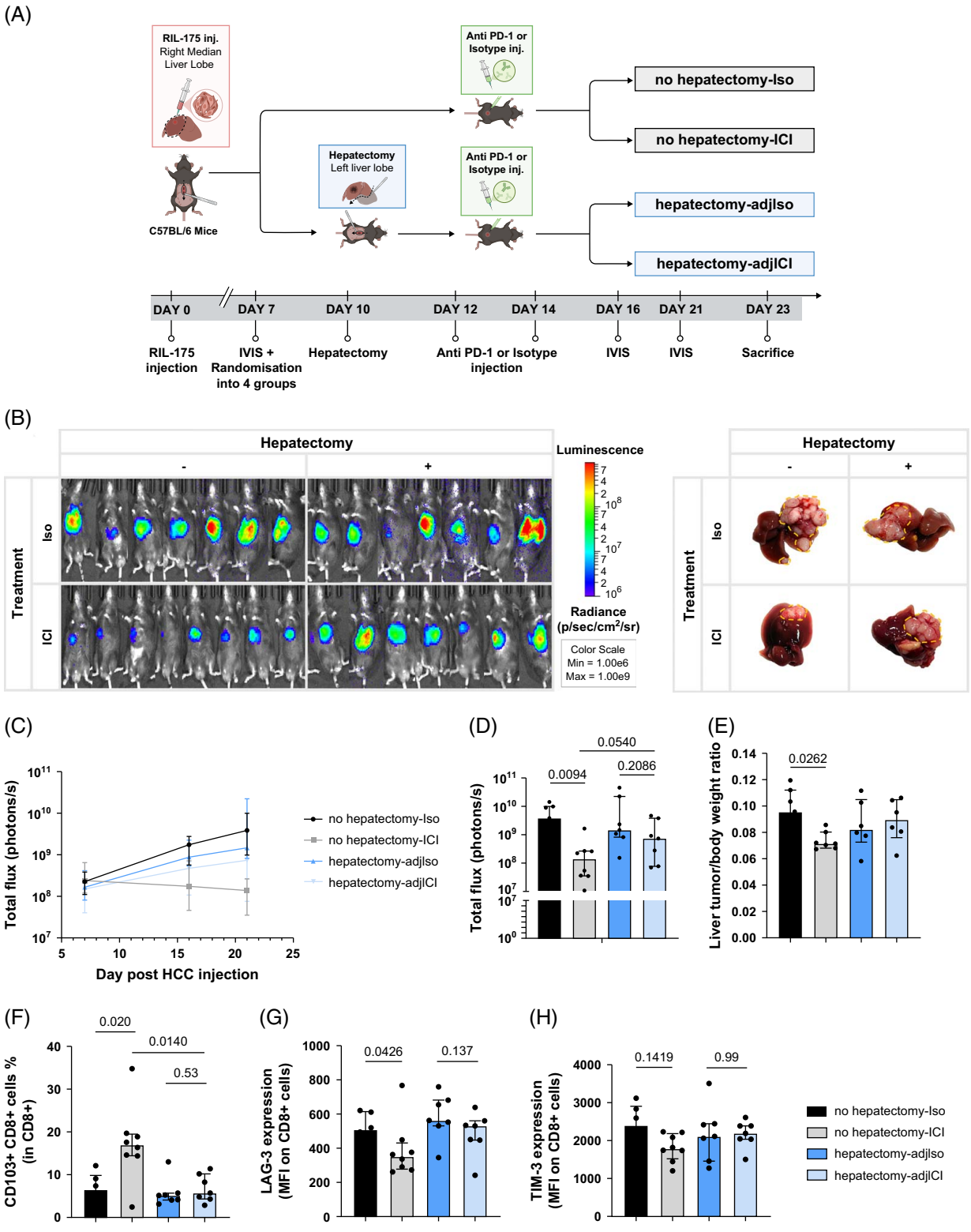

FIGURE 1 Hepatectomy altered adjuvant ICI therapy. (A) Schematic of the experimental workflow. C57BL/6 HCC-bearing mice were left without treatment (no hepatectomy-Iso, black), were treated with ICI (hepatectomy-ICI, gray), underwent a hepatectomy without treatment (hepatectomy-adjIso, dark blue), or underwent a hepatectomy with ICI adjuvant therapy (hepatectomy-adjICI, light blue). (B) Bioluminescence assessment on day 21 after surgery. (C) HCC growth assessment through luminescence measure (photons/s). (D) HCC tumor burden assessment through luminescence measure at day 21 (photons/s). (E) Liver-tumor/body weight ratio on day 21. (F) Percentage of $CD103^+$ $CD8^+$ cells in the tumor. (G, H) LAG-3 and TIM-3 MFI on $CD62L^{low}$ $CD44^+$ $CD8^+$ T cells from tumors. Sample sizes (n per group) are provided in Supplemental Table S2, http://links.lww.com/HEP/K302. Abbreviations: ICI, immune checkpoint inhibitor; MFI, mean fluorescence intensity.

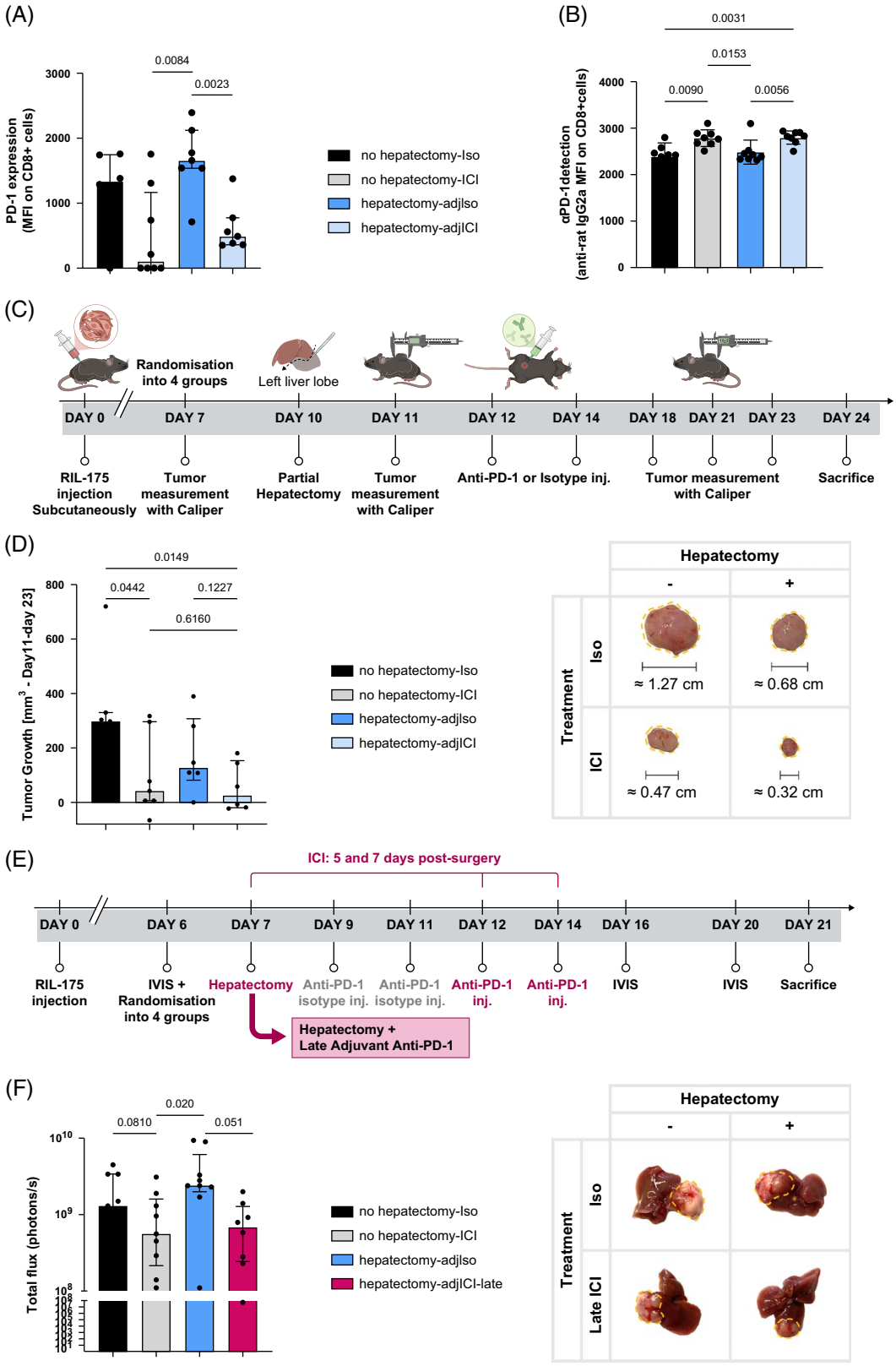

FIGURE 2 Alteration of adjuvant ICI therapy by hepatectomy is not linked to antibody delivery, is liver-specific, and can be restored by a delayed ICI therapy after surgery. (A) PD-1 MFI on CD62L^{low} CD44^{+} CD8^{+} T cells from tumors (no hepatectomy-Iso [black], no hepatectomy-ICI [gray], hepatectomy-adjIso [dark blue], and hepatectomy-adjICI [light blue]). (B) Detection of anti–PD-1 (rat-IgG2a) on CD8^{+} T cells from tumors (no hepatectomy-Iso [black], no hepatectomy-ICI [gray], hepatectomy-adjIso [dark blue], and hepatectomy-adjICI [light blue]). (C, D) Tumor growth of subcutaneously injected HCC in mice without treatment (black), with ICI therapy (gray), with hepatectomy and isotype (dark blue), or with hepatectomy and ICI therapy (light blue). (E, F) HCC tumor burden assessment through luminescence measure (photons/s) (no hepatectomy-Iso

[black], no hepatectomy-ICI [gray], hepatectomy-adjIso [dark blue], and hepatectomy-adjICI_late [violet]). Sample sizes (n per group) are provided in Supplemental Table S1, http://links.lww.com/HEP/K302. Abbreviations: ICI, immune checkpoint inhibitor; MFI, mean fluorescence intensity; PD-1, programmed cell death protein 1.

(RMP1-30) differs from the therapeutic clone (RMP1-14), the decreased MFI may reflect the receptor being occupied by the treatment antibody, leading to epitope masking.[22]

To determine whether the impaired efficacy of adjuvant ICI therapy following surgery was due to an altered antibody delivery, we assessed the presence of anti–PD-1 antibodies on $CD8^+$ TILs using an anti-rat IgG2a. Anti–PD-1 antibodies (rat IgG2a) are present in $CD8^+$ TILs in the ICI-treated groups (Figure 2B), suggesting that the impaired ICI efficacy after hepatectomy was not due to a reduced antibody bioavailability or delivery.

The altered adjuvant anti–PD-1 efficacy after surgery is liver-specific and restored by delaying ICI

To determine whether the surgical effect was liver-specific or systemic, we designed an experiment where we injected RIL-175 cells subcutaneously, followed by partial hepatectomy and anti–PD-1 treatment, and monitored tumor size (Figure 2C). In this model, anti–PD-1 therapy reduced tumor growth irrespective of surgery (Figure 2D), indicating that the surgery did not have an impact on the anti–PD-1 efficacy as it did in the orthotopic model, and that its effect is liver-specific rather than systemic.

Furthermore, to investigate whether delaying the timing of ICI administration could overcome the post-operative immune suppression, we introduced a delayed anti–PD-1 treatment group with injections 5 and 7 days after hepatectomy, compared with 2 and 4 days in the original experiment (Figures 1A and 2E). A reduction in tumor burden was observed in the treated groups ($p = 0.051$ hepatectomy-adjIso vs. hepatectomy-adjICI-late; Figure 2F), which had not been observed with the early adjuvant ICI group before (Figure 1D). This suggests that adjusting the timing of adjuvant treatment with a delayed administration restores its therapeutic benefit.

Hepatectomy alters myeloid cells and impacts anti–PD-1 efficacy

To explore the immune mechanisms behind the impaired efficacy of adjuvant anti–PD-1 therapy following partial hepatectomy, we explored changes in tumor-infiltrating myeloid populations. The results indicated a significant reduction in total conventional dendritic cells (cDCs), including both cDC1 ($CD11c^+$, $MHCII^+$, $CD103^+$) and cDC2 ($CD11c^+$, $MHCII^+$, $CD11b^+$) subsets after hepatectomy, compared with no-hepatectomy, irrespective of ICI treatment (Figure 3A). Similarly, M1-like proinflammatory macrophages ($F4/80^+$, $CD11b^+$, $INOS^+$) were significantly decreased following hepatectomy (Figure 3B), suggesting that surgical intervention affects key antigen-presenting cell populations within the TME, potentially impairing T-cell priming and effector function.

In contrast, plasmacytoid dendritic cells (pDC, $CD11c^+$, $MHCII^+$, $SiglecH^+$) were significantly increased in the surgery ICI-treated group (Figure 3C). This cell population is known to secrete type I interferons (IFN-I) and IL-10 and has been implicated in recruiting myeloid-derived suppressor cells (MDSCs) and promoting immune tolerance after hepatectomy.[1,23] Consistently, a significant increase in ($CD11b^+$, $Ly6C^+$, $Ly6G^+$) MDSCs was observed in the tumors of surgery-treated mice, regardless of ICI treatment ($p = 0.0055$; $p = 0.0024$; Figure 3D).

Together, these results demonstrate that surgery alone alters the tumor-infiltrating myeloid compartment toward a more immunosuppressive and less stimulatory profile, which may contribute to the observed failure of ICI therapy in the adjuvant setting.

To further investigate whether targeting the altered myeloid compartment could rescue the impaired efficacy of adjuvant ICI therapy, we performed a $Ly6C^+$/$Ly6G^+$ cell depletion experiment using the anti-Gr1 antibody (Figure 3E). The combination of anti-Gr1 and anti–PD-1 significantly reduced tumor burden compared with untreated controls ($p = 0.0084$; Figures 3F and G), suggesting that anti-Gr1 depletion restores the efficacy of anti–PD-1 treatment after hepatectomy.

Importantly, anti-Gr1 treatment led to a marked reduction in the frequency of MDSCs ($CD11b^+$, $Ly6C^+$, $Ly6G^+$) and a reduction in pDCs ($CD11c^+$, $MHCII^+$, $SiglecH^+$) compared with mice receiving adjuvant ICI alone ($p = 0.0344$ and $p = 0.0008$, Figures 3H and I). However, no consistent rescue was observed in the levels of cDCs or M1-like macrophages (data not shown).

In addition to $Ly6G^+$ $Ly6C^+$ MDSC, we also observed a marked accumulation of Ly6G- $Ly6C^+$ (monocytic cells) following hepatectomy compared to non-hepatectomy groups ($p = 0.0013$, 0.0033; Supplementary Figure 3, http://links.lww.com/HEP/K302), independent of anti-PD-1 treatment. This population was not significantly reduced by anti-Gr1 myeloid cells depletion, consistent with anti-Gr1 primarily targeting $Ly6G^+$ cells, suggesting that monocytic MDSC represent a distinct surgery-induced immunosuppressive subset.

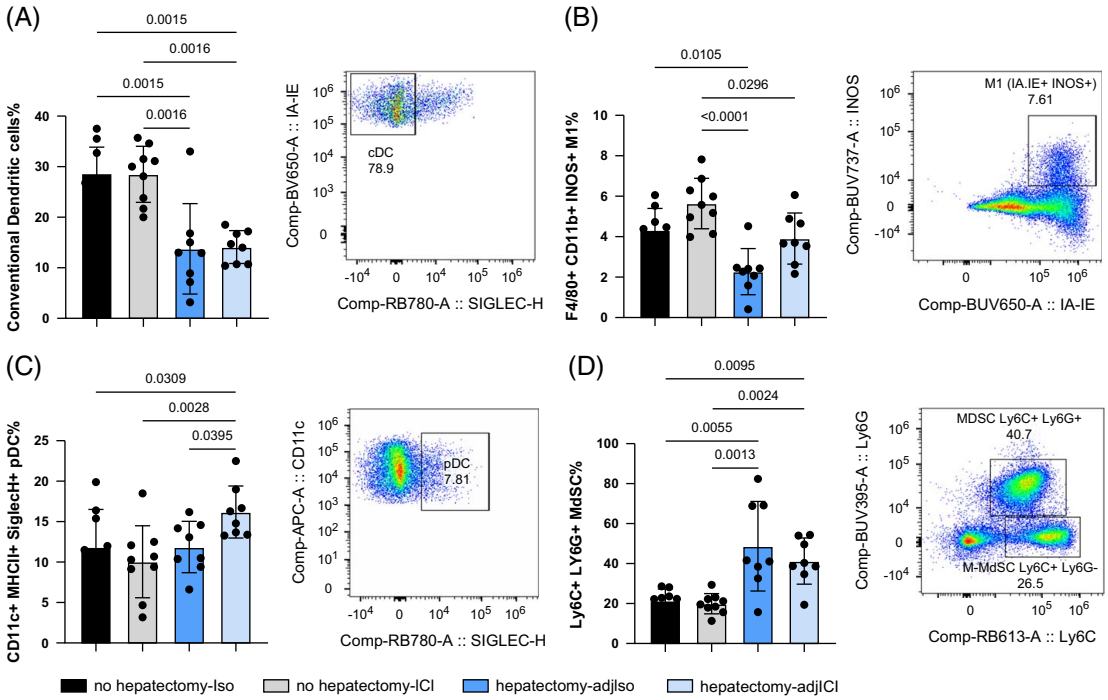

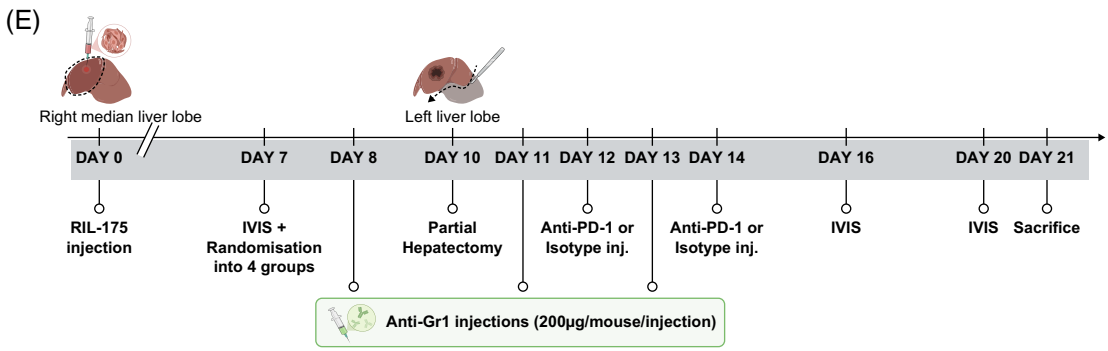

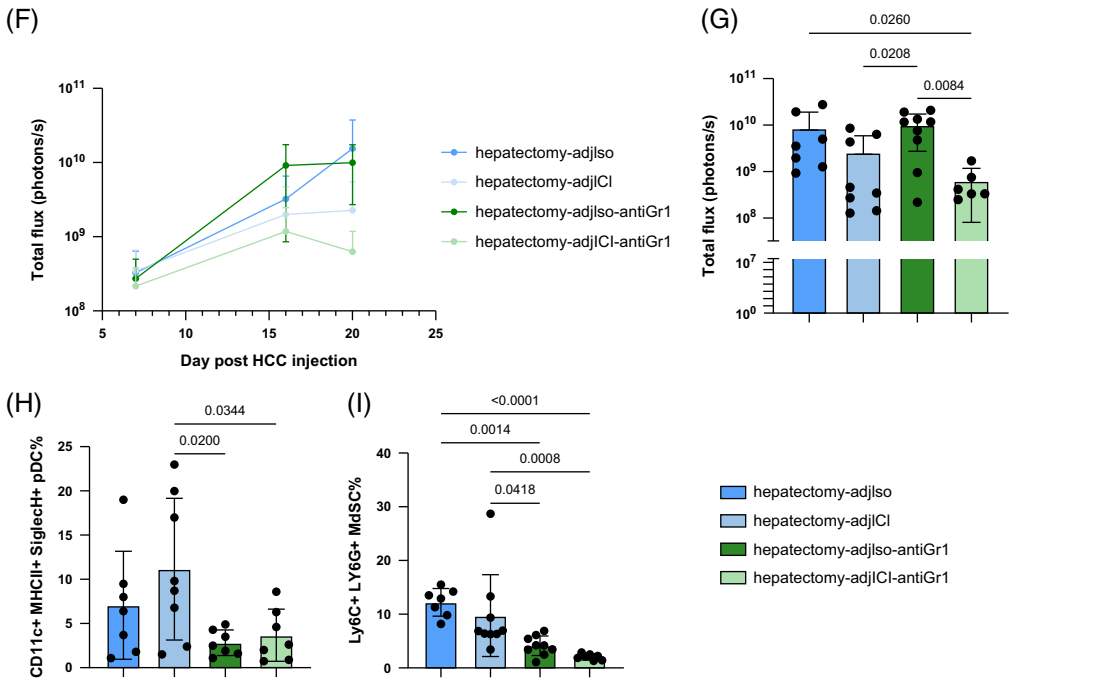

FIGURE 3 Hepatectomy altered the myeloid compartment. HCC-bearing mice were left without treatment (no hepatectomy-Iso, black), were treated with ICI (no hepatectomy-ICI, gray), underwent a hepatectomy without treatment (hepatectomy-adjIso, dark blue), or underwent a hepatectomy with ICI adjuvant therapy (hepatectomy-adjICI, light blue). (A–D) Percentage of myeloid cell subsets in tumors at day 21. (E) HCC-bearing mice underwent a hepatectomy without treatment (hepatectomy-adjIso, dark blue), a hepatectomy with ICI adjuvant therapy (hepatectomy-adjICI, light blue), or received anti-Gr1 antibodies and underwent a hepatectomy without treatment (hepatectomy-adjIso-anti-Gr1, dark green), or with ICI adjuvant therapy (hepatectomy-adjICI-anti-Gr1, light green). (F) HCC growth assessment through luminescence measure (photons/s). (G) Bioluminescence assessment on day 20 after surgery (photons/s). (H, I) Percentage of myeloid cell subsets in the tumors on day 21. Sample sizes (n per group) are provided in Supplemental Table S2, http://links.lww.com/HEP/K302. Abbreviation: ICI, immune checkpoint inhibitor.

Together, these results support the hypothesis that hepatectomy-induced accumulation of immunosuppressive myeloid cells, particularly MDSCs and pDCs, compromises the efficacy of adjuvant anti–PD-1 therapy.

Anti–PD-1 efficacy is restored when using neoadjuvant compared with adjuvant

As shown previously in our model, hepatectomy impairs adjuvant ICI treatment. Shifting immunotherapy to the neoadjuvant setting (before surgery) has been shown to enhance treatment responses and survival in other solid tumors.[24] We designed a similar orthotopic murine HCC model and introduced 2 additional experimental groups receiving either anti–PD-1 antibodies or isotype controls 2 and 4 days before the surgery (Figure 4A).

Mice treated with anti–PD-1 before hepatectomy (neoadjuvant setting) demonstrated a significantly reduced tumor size compared with isotype controls ($p = 0.0005$; Figure 4B). This tumor size reduction was not observed when ICI was administered after hepatectomy (Figure 4B). Liver mass-to-body weight ratios have also shown consistent results with a significant reduction in the neoadjuvant ICI group ($p = 0.0411$; Figure 4C). Similarly, histological analysis of liver sections confirmed these results as tumor areas were significantly reduced in neoadjuvant ICI-treated mice ($p = 0.0088$; Figure 4D).

Immunohistochemistry results of immune profiling of liver sections show a significant increase in infiltrated $CD45^+$ cells in livers of mice receiving neoadjuvant anti–PD-1 (Figure 4E), suggesting enhanced immune cell recruitment and migration to the TME. This effect was not observed in the adjuvant setting, suggesting that initiating immune modulation before surgery may reduce the immunosuppressive effects induced by surgery.

Neoadjuvant anti–PD-1 improves cytotoxic T-cell immunity

To further investigate the impact of neoadjuvant ICI on the TME, we evaluated $CD8^+$ T-cell infiltration and activation in liver tumors. Flow cytometry analysis revealed a significantly higher percentage of $CD103^+CD8^+$ T cells in tumors of mice treated with neoadjuvant anti–PD-1 compared with those left untreated ($p = 0.024$; Figure 5A), suggesting improved tissue residency and potentially cytotoxicity. Quantitative PCR on the tumor revealed an increased expression of Cd8 after ICI treatment ($p = 0.0275$; Figure 5B). This increase is lost when the treatment is administered after surgery.

Bulk RNA sequencing of enriched $CD8^+$ T cells isolated from tumors treated with ICI demonstrated an upregulation of key activation and effector genes. The expression of a selection of some of these genes, including Cxcr6, Tbx21, Cd69, Il2ra, and Gzma, was confirmed using quantitative PCR. A significant increase in their expression in the neoadjuvant group was observed compared with the adjuvant ($p = 0.0249$; 0.0266; 0.0241; 0.0185, respectively) and control groups (Figures 5C–G).

The infiltration of $CD8^+$ cells in the group treated with neoadjuvant treatment is more potent in the periphery of the tumor ($p = 0.0236$; Figure 5H) and not in the center of the tumor (data not shown). In addition, fewer tumor lymphatic and vascular invasions were present in the tumors of mice treated with ICI as neoadjuvant or without hepatectomy (Figure 5I), thus corresponding to a decreased tumor aggressiveness.

These findings indicate that neoadjuvant ICI therapy not only enhances $CD8^+$ T-cell infiltration but also promotes a transcriptional program associated with cytotoxicity and effector function, supporting its superior efficacy in shaping antitumor immunity before surgical resection and thus avoiding vascular invasion.

Neoadjuvant anti–PD-1 improves survival and reduces recurrence after hepatectomy in mice

We further assessed the impact of neoadjuvant versus adjuvant ICI on survival and tumor recurrence. Using the previously established orthotopic HCC model, a curative partial hepatectomy was this time performed with resection of the tumor-bearing lobe. Tumor growth was monitored using IVIS, and mice were followed for survival and recurrence until sacrifice on day 70 after injection (Figure 6A).

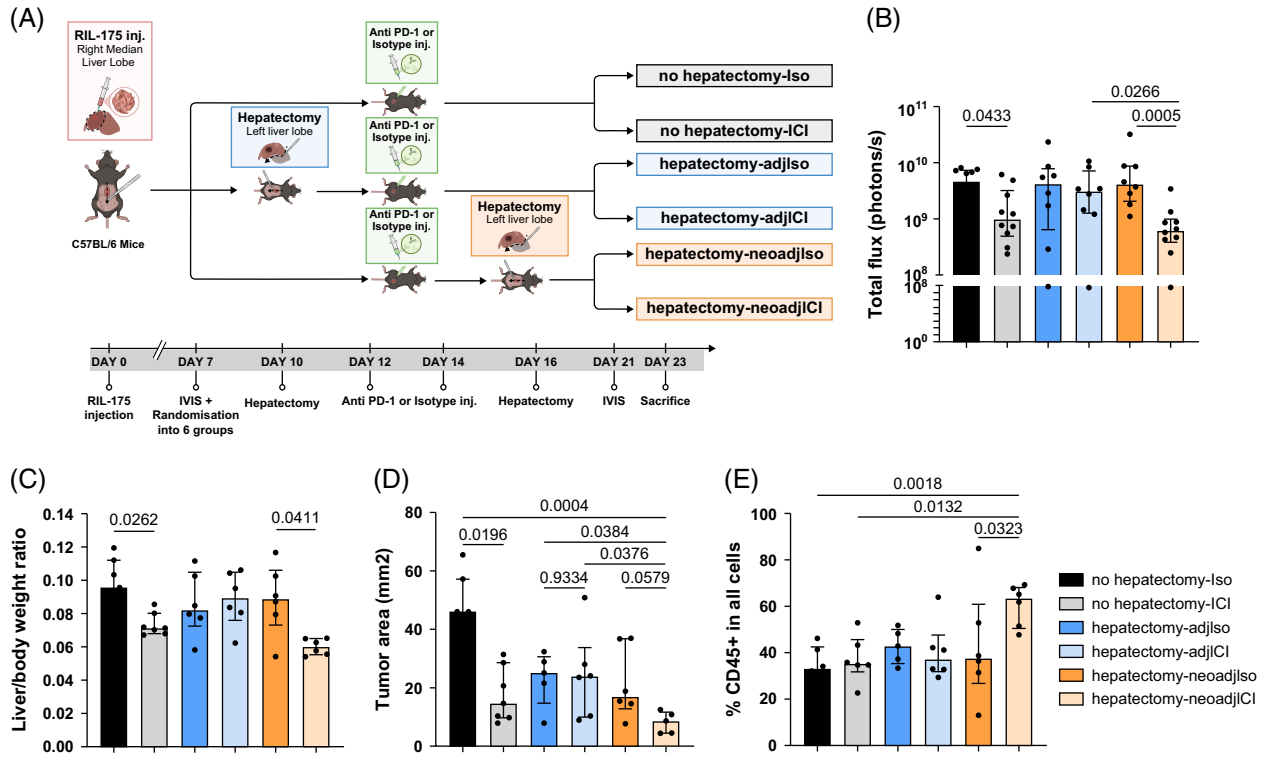

FIGURE 4 ICI therapy efficacy is restored when used as a neoadjuvant before hepatectomy. (A) HCC-bearing mice were left without treatment (no hepatectomy-Iso, black), were treated with ICI (no hepatectomy-ICI, gray), underwent a hepatectomy without treatment (hepatectomy-adjIso, dark blue) or with ICI adjuvant therapy (hepatectomy-adjICI, light blue), underwent a hepatectomy without treatment (hepatectomy-neoadjIso, dark orange) or with ICI neoadjuvant therapy (hepatectomy-neoadjICI, light orange). (B) HCC tumor burden assessment through luminescence measure at day 21 (photons/s). (C) Liver-tumor/body weight ratio at day 23. (D) Tumor area (mm^2) assessment on liver tumor sections. (E) $CD45^+$ cells assessment on liver tumor sections. Sample sizes (n per group) are provided in Supplemental Table S2, http://links.lww.com/HEP/K302. Abbreviation: ICI, immune checkpoint inhibitor.

Kaplan-Meier survival analysis demonstrated a significant prolonged survival in the neoadjuvant anti–PD-1 group compared with the isotype control group ($p = 0.0373$), while the adjuvant anti–PD-1 group did not show a statistically significant improvement (Figure 6B).

The assessment of tumor recurrence via IVIS and its confirmation at sacrifice revealed that neoadjuvant anti–PD-1 treatment significantly reduced recurrence compared with the isotype group ($p = 0.0405$; Figure 6C). In contrast, its administration in the adjuvant setting failed to reduce recurrence and was associated with a higher incidence of tumor relapses relative to the control group. In addition, no extrahepatic recurrences were found in the neoadjuvant ICI group, while 5 pulmonary recurrences were found in the adjuvant ICI group ($p = 0.053$; Figure 6D). This suggests that administering anti–PD-1 therapy before surgical resection enhances the immune control against minimal residual disease and extends survival in this murine HCC model.

DISCUSSION

The integration of ICIs in the surgical management of early-stage HCC is emerging as a promising strategy to improve curative outcomes. Our study provides mechanistic and functional evidence that the timing of anti–PD-1 administration critically influences treatment efficacy in the context of partial hepatectomy. Using an orthotopic murine model of HCC, we demonstrate that neoadjuvant, but not adjuvant, anti–PD-1 immunotherapy improves tumor control, reduces recurrence, and significantly extends survival following curative hepatectomy.

While anti–PD-1 therapy was effective in non-surgical settings, its efficacy was lost when administered in the adjuvant setting after hepatectomy. This loss of effect was not due to impaired antibody delivery or systemic immunosuppression but rather linked to surgery-induced alterations in the liver-specific TME, especially in the myeloid compartment. In the settings of surgery, pDCs have been implicated in HCC recurrence through the recruitment of MDSCs via IFN-α secretion.[25] After partial hepatectomy, liver regeneration is characterized by the infiltration of neutrophils. This increased inflammatory response promotes a protumor niche and increases colorectal metastasis in rodent models.[26] In humans, the accumulation of immunosuppressive MDSCs after surgery was also demonstrated in patients with gastrointestinal cancer.[14] The observations are

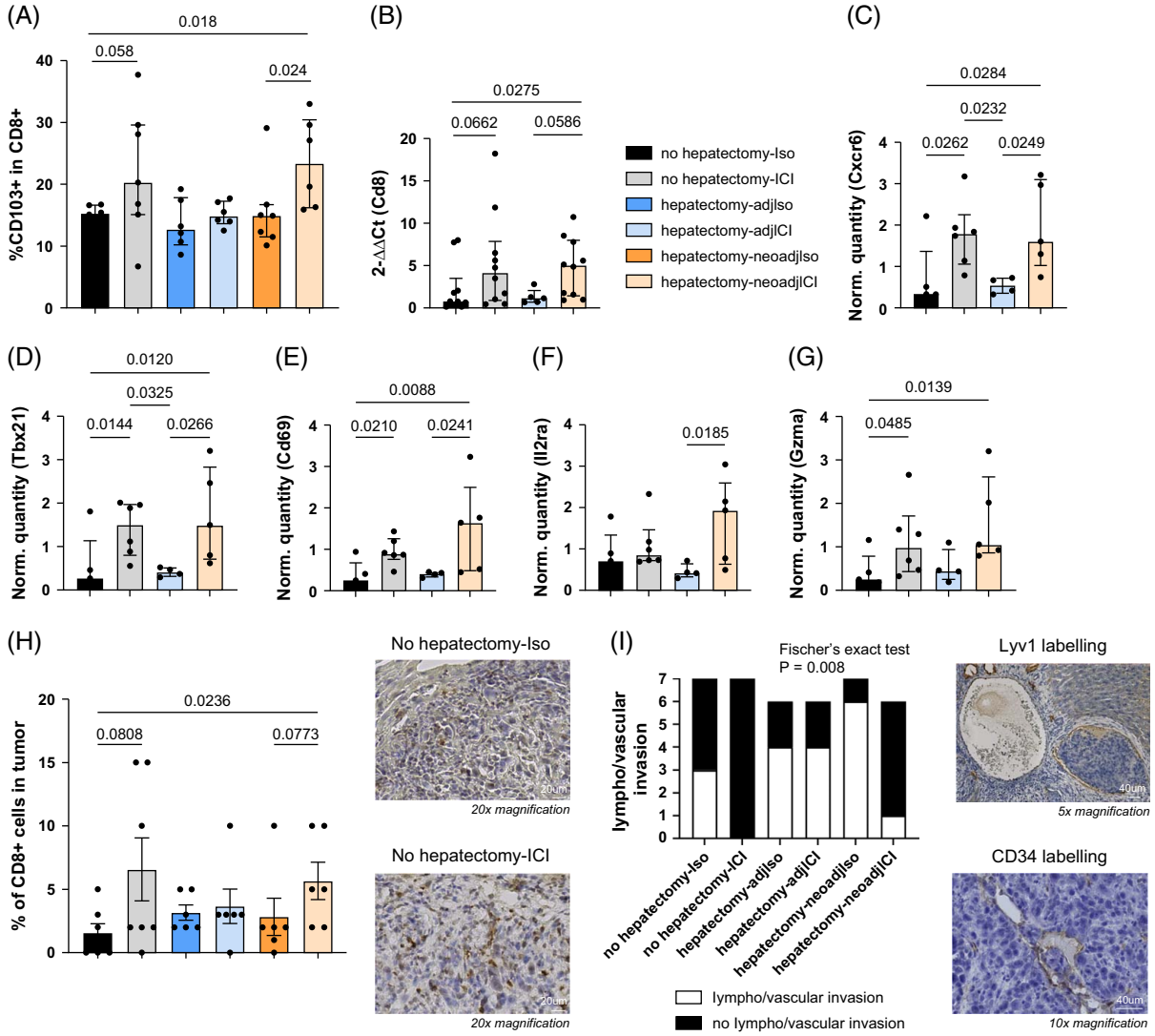

FIGURE 5 Neoadjuvant before hepatectomy improves the cytotoxic T-cell immunity compared with ICI administered adjuvantly. HCC-bearing mice were left without treatment (no hepatectomy-Iso, black), were treated with ICI (no hepatectomy-ICI, gray), underwent a hepatectomy without treatment (hepatectomy-adjIso, dark blue) or with ICI adjuvant therapy (hepatectomy-adjICI, light blue), underwent a hepatectomy without treatment (hepatectomy-neoadjIso, dark orange) or with ICI neoadjuvant therapy (hepatectomy-neoadjICI, light orange). (A) Percentage of $CD103^+$ $CD8^+$ in the tumor on day 21. (B) CD8 expression in tumors at day 21. (C–G) Gene expression (Cxcr6, Tbx21, Cd69, Il2ra, and Gzma) on $CD8^+$ T cells sorted from tumors on day 21. (H) Percentage of $CD8^+$ cells in the periphery of the tumor (left: quantification, right: representative pictures). (I) Lymphatic and vascular invasion in the tumor (left: evaluation (yes/no), right: representative pictures). Sample sizes (n per group) are provided in Supplemental Table S2, http://links.lww.com/HEP/K302. Abbreviation: ICI, immune checkpoint inhibitor.

similar in our experiments, notably with a reduction of key antigen-presenting cells, including cDC1 and M1-like macrophages, and the accumulation of immunosuppressive pDCs and MDSCs after hepatectomy. In addition, the functional relevance of these changes was confirmed by MDSC depletion with anti-Gr1, which restored adjuvant anti–PD-1 efficacy, reduced pDC accumulation, and partially reversed the immunosuppressive TME. This underlines the role of the myeloid compartment as a dominant regulator of postoperative immune competence.

Therefore, hepatectomy suppressed the infiltration of $CD103^+CD8^+$ tissue-resident memory T cells, and this shift correlates with increased expression of exhaustion markers such as LAG-3 and TIM-3, consistent with previous reports of surgery-induced immune dysfunction.[27] In contrast, neoadjuvant ICI administration preserved and enhanced $CD8^+$ T-cell infiltration and activation. RNA sequencing and qPCR analyses of tumor-infiltrating $CD8^+$ T cells revealed upregulation of cytotoxic effectors (Gzma), transcription factors (Tbx21), and cell activation and migration markers (Cd69 and Cxcr6), indicating robust immune activation. This translated into significantly lower recurrence rates and superior survival compared with both adjuvant and control groups.

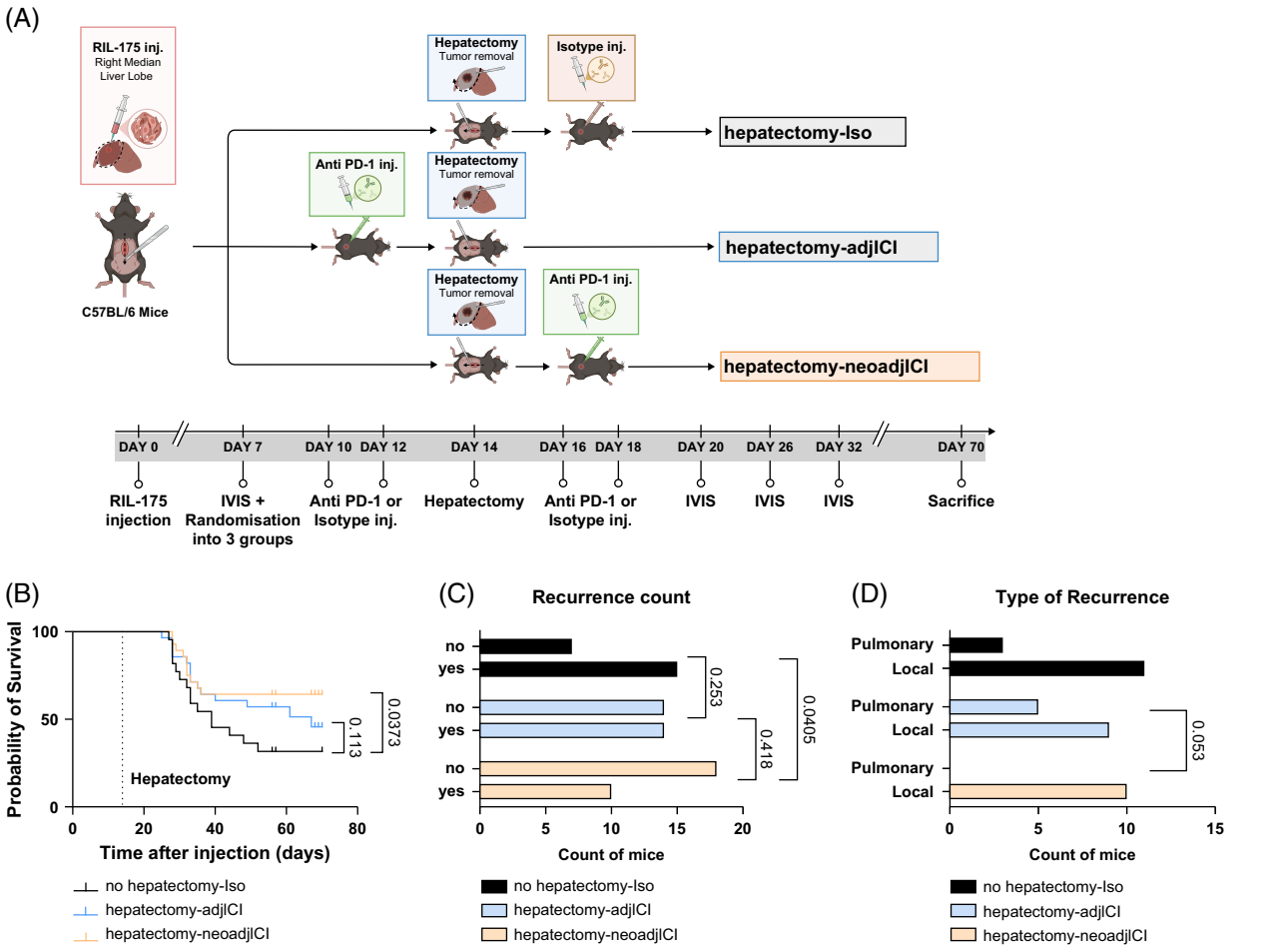

FIGURE 6 Recurrence risk after hepatectomy decreases with neoadjuvant ICI therapy. (A) HCC-bearing mice underwent a curative hepatectomy without treatment (no hepatectomy-Iso, black), with adjuvant ICI (hepatectomy-adjICI, blue), or with neoadjuvant ICI (hepatectomy-neoadjICI, orange). (B) Probability of survival after curative hepatectomy. (C) Recurrence counts after curative hepatectomy. (D) Type of recurrence after curative hepatectomy. Sample sizes (n per group) are provided in Supplemental Table S2, http://links.lww.com/HEP/K302. Abbreviation: ICI, immune checkpoint inhibitor.

In HCC, vascular invasion is a major risk factor for intrahepatic metastasis and early recurrence after resection.[28,29] In our experiments, in addition to an improved infiltration of effector memory $CD8^+$ T cells ($CD103^+$) with an activated phenotype, neoadjuvant ICI-treated HCC have a decreased number of lymphatic and vascular tumor invasion. This finding correlates with the lower HCC recurrences and the absence of pulmonary recurrence in the neoadjuvant-treated group (Figure 6). Of note, the efficacy of neoadjuvant ICI to prevent HCC recurrence in the curative hepatectomy model may also be a consequence of a decreased tumor burden before surgery, leading to a less complex hepatectomy and a lower release of tumor cells.

These findings align with observations in other solid tumors, where neoadjuvant ICI creates superior systemic and memory T-cell responses compared with adjuvant approaches. In murine breast cancer and lung cancer models, neoadjuvant ICI elicits more robust systemic and memory T-cell responses compared with adjuvant therapy.[24] In the clinical setting, the CheckMate 816 trial in non–small cell lung cancer demonstrated improved pathologic response and event-free survival with preoperative ICI.[15,30] Early-phase studies in HCC also suggest that neoadjuvant PD-1 blockade can foster favorable immune remodeling of the TME.[16,31] Collectively, these data support the hypothesis of the immunologic cost of tumor resection, where surgery not only removes tumor antigen sources but also induces organ-specific immunosuppression that may blunt the efficacy of adjuvant immunotherapies.

Among the limitations of this study are the use of a single tumor cell line, the absence of combination regimens (such as anti-VEGF + ICI), and the choice of the murine model without underlying liver disease that does not fully reflect the complex nature of HCC pathologies in patients.

The RIL-175 HCC cell line is an anti–PD-1 responsive model and mimics HCC with a high percentage of T

cells with an inactive phenotype and DC infiltration.[32] This corresponds to HCC classified as the inflamed immune class, which represents 35% of HCC cases.[33] The TME of the inflamed HCC class may have a specific response to hepatectomy with the migration of suppressive myeloid cells and pDCs that is not representative of all HCC classes. However, the inflamed class of HCC being the most suspected to represent potential responders to ICI therapies, tumors belonging to this class were the most interesting to investigate.[34]

A potential limitation of our model is that luciferase expression, as with other foreign reporter proteins, may provoke an immune response, which might influence tumor growth kinetics. Although our principal findings are supported by independent measurements beyond bioluminescence, we acknowledge that immunogenicity of the luciferase reporter could partially contribute to variability in outcomes, and this should be considered in interpreting the results.

Our experiments evaluated anti–PD-1 as monotherapy. While this allowed a clean dissection of timing effects, it does not reflect current therapeutic standards.[4] Multiple clinical trials have established that the immunologic activity of ICI in HCC is significantly enhanced when combined with antiangiogenic agents; anti-VEGF can reduce abnormal neovascularization, alleviate hypoxia, improve dendritic cell priming, and decrease recruitment of MDSCs and Tregs.[35–37] However, the use of VEGF inhibitors carries risks, as these agents impair endothelial repair, angiogenesis, and wound healing if not appropriately timed.[38]

Finally, our model was based on partial hepatectomy in otherwise healthy mice. Epidemiological data indicate that $>80\%$–90% of human HCC develops in the context of chronic liver disease, including viral hepatitis, alcohol-associated liver diseases, and metabolic dysfunction–associated liver diseases.[39,40] Cirrhosis and fibrosis remodel sinusoidal vasculature, increase extracellular matrix stiffness, and alter immune cell trafficking, creating physical and immunologic barriers to effector T-cell infiltration.[41] Moreover, chronic antigenic stimulation in inflamed livers drives T-cell exhaustion and suppressive myeloid expansion, all of which attenuate ICI efficacy.[42] Notably, recent work in murine NASH-HCC models demonstrated that metabolic inflammation promotes the accumulation of $CXCR2^{+}$ neutrophils, driving resistance to anti–PD-1 despite tumor immunogenicity.[43] Thus, the absence of fibrosis or chronic liver injury in our model may underestimate the barriers to ICI efficacy that are encountered in human HCC.

Altogether, future studies will investigate whether these findings hold across different HCC classes, combination therapies, and murine models with an advanced stage of liver disease.

In conclusion, this work identifies postoperative myeloid-driven immunosuppression as a key barrier to adjuvant PD-1 efficacy in HCC and provides preclinical evidence that neoadjuvant ICI offers superior tumor control, immune activation, and survival benefit compared with postoperative administration.

DATA AVAILABILITY STATEMENT

Data will be available at the time of publication in the institutional repository https://doi.org/10.26037/yareta:53eg74ujvbedvpdh2ynsxbd4fy.

AUTHOR CONTRIBUTIONS

Conceptualization: Stéphanie Lacotte and Christian Toso; methodology: Roqiya Bouguerra, Sofia El Hajji, and Stéphanie Lacotte; investigation: Roqiya Bouguerra, Sofia El Hajji, Charles-Henri Wassmer, Arnaud Bakaric, Florence Slits, and Stéphanie Lacotte; writing—original draft: Roqiya Bouguerra and Stéphanie Lacotte; writing—review/editing: Arnaud Bakaric, Beat Moeckli, Laura Rubbia-Brandt, and Christian Toso; funding acquisition: Christian Toso.

ACKNOWLEDGMENTS

The authors thank the personnel of the Genomic Core Facility of the Faculty of Medicine (University of Geneva), the Histology Core Facility of the Faculty of Medicine (University of Geneva), and the Flow Cytometry Core Facility of the Faculty of Medicine (University of Geneva). They especially thank Jean Pierre Giliberto and Raphaël Ruttimann for their help with IVIS imaging. Parts of Figure 1-4 and Visual Abstract were created using BioRender.com.

FUNDING INFORMATION

The Fond'Action contre le cancer and the Ligue Suisse Contre le Cancer funded this research. Roqiya Bouguerra is supported by the Swiss Government Excellence Scholarship.

CONFLICTS OF INTEREST

The authors have no conflicts to report.

ORCID

Sofia El Hajji https://orcid.org/0000–0002–3028–6148
Stéphanie Lacotte https://orcid.org/0000–0002–5921–6389

REFERENCES

1. Seyhan D, Allaire M, Fu Y, Conti F, Wang XW, Gao B, et al. Immune microenvironment in hepatocellular carcinoma: From pathogenesis to immunotherapy. Cell Mol Immunol. 2025;22:1132–58.
2. Liu Z, Lin Y, Zhang J, Zhang Y, Li Y, Liu Z, et al. Molecular targeted and immune checkpoint therapy for advanced hepatocellular carcinoma. J Exp Clin Cancer Res. 2019;38:447.
3. Llovet JM, Ricci S, Mazzaferro V, Hilgard P, Gane E, Blanc JF, et al. Sorafenib in advanced hepatocellular carcinoma. N Engl J Med. 2008;359:378–90.

4. Finn RS, Qin S, Ikeda M, Galle PR, Ducreux M, Kim TY, et al. Atezolizumab plus bevacizumab in unresectable hepatocellular carcinoma. N Engl J Med. 2020;382:1894–905.
5. Abou-Alfa GK, Lau G, Kudo M, Chan SL, Kelley RK, Furuse J, et al. Tremelimumab plus durvalumab in unresectable hepatocellular carcinoma. NEJM Evid. 2022;1:EVIDoa2100070.
6. Qin S, Chan SL, Gu S, Bai Y, Ren Z, Lin X, et al. Camrelizumab plus rivoceranib versus sorafenib as first-line therapy for unresectable hepatocellular carcinoma (CARES-310): A randomised, open-label, international phase 3 study. Lancet Lond Engl. 2023;402:1133–46.
7. Tabrizian P, Marino R, Chow PKH. Liver resection and transplantation in the era of checkpoint inhibitors. JHEP Rep. 2024;6:101181.
8. Mittendorf EA, Burgers F, Haanen J, Cascone T. Neoadjuvant immunotherapy: Leveraging the immune system to treat early-stage disease. Am Soc Clin Oncol Educ Book. 2022;42:189–203.
9. Bray F, Laversanne M, Sung H, Ferlay J, Siegel RL, Soerjomataram I, et al. Global cancer statistics 2022: GLOBOCAN estimates of incidence and mortality worldwide for 36 cancers in 185 countries. CA Cancer J Clin. 2024;74:229–63.
10. Wang K, Xiang YJ, Yu HM, Cheng YQ, Liu ZH, Qin YY, et al. Adjuvant sintilimab in resected high-risk hepatocellular carcinoma: A randomized, controlled, phase 2 trial. Nat Med. 2024;30:708–15.
11. Yopp A, Kudo M, Chen M, Cheng AL, Kaseb AO, Lee HC, et al. LBA39 Updated efficacy and safety data from IMbrave050: Phase III study of adjuvant atezolizumab (atezo) + bevacizumab (bev) vs active surveillance in patients (pts) with resected or ablated high-risk hepatocellular carcinoma (HCC). Ann Oncol. 2024;35:S1230.
12. Bezu L, Akçal Öksüz D, Bell M, Buggy D, Diaz-Cambronero O, Enlund M, et al. Perioperative immunosuppressive factors during cancer surgery: An updated review. Cancers. 2024;16:2304.
13. Patel SP, Othus M, Chen Y, Wright GP, Yost KJ, Hyngstrom JR, et al. Neoadjuvant–adjuvant or adjuvant-only pembrolizumab in advanced melanoma. N Engl J Med. 2023;388:813–23.
14. Tang F, Tie Y, Tu C, Wei X. Surgical trauma-induced immunosuppression in cancer: Recent advances and the potential therapies. Clin Transl Med. 2020;10:199–223.
15. Forde PM, Spicer J, Lu S, Provencio M, Mitsudomi T, Awad MM, et al. Neoadjuvant nivolumab plus chemotherapy in resectable lung cancer. N Engl J Med. 2022;386:21.
16. D'Alessio A, Stefanini B, Blanter J, Adegbite B, Crowley F, Yip V, et al. Pathological response following neoadjuvant immune checkpoint inhibitors in patients with hepatocellular carcinoma: A cross-trial, patient-level analysis. Lancet Oncol. 2024;25:1465–75.
17. Kaseb A, Hasanov E, Cao T, Shen Y, Vauthey JN, Lee SY, et al. Perioperative nivolumab monotherapy versus nivolumab plus ipilimumab in resectable hepatocellular carcinoma: A randomised, open-label, phase 2 trial. Lancet Gastroenterol Hepatol. 2022;7:208–18.
18. Yu SJ, Ma C, Heinrich B, Brown ZJ, Sandhu M, Zhang Q, et al. Targeting the crosstalk between cytokine-induced killer cells and myeloid-derived suppressor cells in hepatocellular carcinoma. J Hepatol. 2019;70:449–57.
19. Zender L, Xue W, Cordón-Cardo C, Hannon GJ, Lucito R, Powers S, et al. Generation and analysis of genetically defined liver carcinomas derived from bipotential liver progenitors. Cold Spring Harb Symp Quant Biol. 2005;70:251–61.
20. Kwong TT, Xiong Z, Zhang Y, Wu H, Cao J, Pak-Chun Wong P, et al. Overcoming immunotherapy resistance in hepatocellular carcinoma by targeting myeloid IL-8/CXCR2 signaling. Mol Ther J Am Soc Gene Ther. 2025;33:1659–73.
21. Nose Y, Saito T, Yamamoto K, Yamashita K, Tanaka K, Yamamoto K, et al. The tissue-resident marker CD103 on peripheral blood T cells predicts responses to anti-PD-1 therapy in gastric cancer. Cancer Immunol Immunother CII. 2023;72:169–81.
22. Bu MT, Yuan L, Klee AN, Freeman GJ. A comparison of murine PD-1 and PD-L1 monoclonal antibodies. Monoclon Antibodies Immunodiagn Immunother. 2022;41:202–9.
23. She S, Shi J, Zhu J, Yang F, Yu J, Dai K. Impact of inflammation and the immune system on hepatocellular carcinoma recurrence after hepatectomy. Cancer Med. 2024;13:e7018.
24. Liu J, Blake SJ, Yong MCR, Harjunpää H, Ngiow SF, Takeda K, et al. Improved efficacy of neoadjuvant compared to adjuvant immunotherapy to eradicate metastatic disease. Cancer Discov. 2016;6:1382–99.
25. Pang L, Yeung OWH, Ng KTP, Liu H, Zhu J, Liu J, et al. Postoperative plasmacytoid dendritic cells secrete IFNα to promote recruitment of myeloid-derived suppressor cells and drive hepatocellular carcinoma recurrence. Cancer Res. 2022;82:4206–18.
26. Luenstedt J, Hoping F, Feuerstein R, Mauerer B, Berlin C, Rapp J, et al. Partial hepatectomy accelerates colorectal metastasis by priming an inflammatory premetastatic niche in the liver. Front Immunol. 2024;15:1388272.
27. Plunkett KR, Armitage JD, Inderjeeth AJ, McDonnell AM, Waithman J, Lau PKH. Tissue-resident memory T cells in the era of (Neo) adjuvant melanoma management. Front Immunol. 2022;13:1048758.
28. Mazzaferro V, Llovet JM, Miceli R, Bhoori S, Schiavo M, Mariani L, et al. Predicting survival after liver transplantation in patients with hepatocellular carcinoma beyond the Milan criteria: A retrospective, exploratory analysis. Lancet Oncol. 2009;10:35–43.
29. Lim KC, Chow PKH, Allen JC, Chia GS, Lim M, Cheow PC, et al. Microvascular invasion is a better predictor of tumor recurrence and overall survival following surgical resection for hepatocellular carcinoma compared to the Milan criteria. Ann Surg. 2011;254:108.
30. Crenier R, Duchemann B. [Nivolumab plus chemotherapy in neoadjuvant treatment of NSCLC with PD-L1 expression ≥ 1]. Bull Cancer (Paris). 2024;111:1003–4.
31. Wang J, Cao W, Huang J, Zhou Y, Zheng R, Lou Y, , et al Tumor-associated CD19$^+$ macrophages induce immunosuppressive microenvironment in hepatocellular carcinoma. arXiv; 2025. Available from: http://arxiv.org/abs/2503.17738
32. Zabransky DJ, Danilova L, Leatherman JM, Lopez-Vidal TY, Sanchez J, Charmsaz S, et al. Profiling of syngeneic mouse HCC tumor models as a framework to understand anti-PD-1 sensitive tumor microenvironments. Hepatol Baltim Md. 2023;77:1566–79.
33. Montironi C, Castet F, Haber PK, Pinyol R, Torres-Martin M, Torrens L, et al. Inflamed and non-inflamed classes of HCC: A revised immunogenomic classification. Gut. 2023;72:129–40.
34. Hong JY, Cho HJ, Sa JK, Liu X, Ha SY, Lee T, et al. Hepatocellular carcinoma patients with high circulating cytotoxic T cells and intra-tumoral immune signature benefit from pembrolizumab: Results from a single-arm phase 2 trial. Genome Med. 2022;14:1.
35. Lee WS, Yang H, Chon HJ, Kim C. Combination of anti-angiogenic therapy and immune checkpoint blockade normalizes vascular-immune crosstalk to potentiate cancer immunity. Exp Mol Med. 2020;52:1475–85.
36. Ochoa MC, Sanchez-Gregorio S, de Andrea CE, Garasa S, Alvarez M, Olivera I, et al. Synergistic effects of combined immunotherapy strategies in a model of multifocal hepatocellular carcinoma. Cell Rep Med. 2023;4:101009.
37. Kuo HY, Khan KA, Kerbel RS. Antiangiogenic–immune-checkpoint inhibitor combinations: Lessons from phase III clinical trials. Nat Rev Clin Oncol. 2024;21:468–82.

38. Bailey CE, Parikh AA. Assessment of the risk of antiangiogenic agents before and after surgery. Cancer Treat Rev. 2018;68: 38–46.
39. Moon AM, Singal AG, Tapper EB. Contemporary epidemiology of chronic liver disease and cirrhosis. Clin Gastroenterol Hepatol. 2020;18:2650–66.
40. El-Serag HB. Epidemiology of viral hepatitis and hepatocellular carcinoma. Gastroenterology. 2012;142:1264–73.
41. Somnay K, Wadgaonkar P, Sridhar N, Roshni P, Rao N, Wadgaonkar R. Liver fibrosis leading to cirrhosis: Basic mechanisms and clinical perspectives. Biomedicines. 2024;12: 2229.
42. Provera A, Vecchio C, Sheferaw AN, Stoppa I, Pantham D, Dianzani U, et al. From MASLD to HCC: What's in the middle? Heliyon. 2024;10: e35338.
43. Leslie J, Mackey JBG, Jamieson T, Ramon-Gil E, Drake TM, Fercoq F, et al. CXCR2 inhibition enables NASH-HCC immunotherapy. Gut. 2022;71:2093–106.

How to cite this article: Bouguerra R, El Hajji S, Wassmer C, Bakaric A, Slits F, Moeckli B, et al. Hepatectomy alters adjuvant anti-PD-1 action in a mouse model of HCC but does not compromise neoadjuvant efficacy. Hepatology. 2025;■■:■■–■■. https://doi.org/10.1097/HEP.0000000000001575